Hindawi Publishing Corporation
International Journal of Antennas and Propagation
Volume 2012, Article ID 910824, 9 pages
doi:10.1155/2012/910824

Research Article

Partial PIC-MRC Receiver Design for Single Carrier Block Transmission System over Multipath Fading Channels

Juinn-Horng Deng and Sheng-Yang Huang

Communication Research Center and Department of Communication Engineering, Yuan Ze University, Chungli, Taoyuan 32003, Taiwan

Correspondence should be addressed to Juinn-Horng Deng, jh.deng@saturn.yzu.edu.tw

Received 20 May 2012; Revised 25 July 2012; Accepted 26 July 2012

Academic Editor: Chih-Peng Li

Single carrier block transmission (SCBT) system has become one of the most popular modulation systems due to its low peak-to-average power ratio (PAPR), and it is gradually considered to be used for uplink wireless communication systems. In this paper, a low complexity partial parallel interference cancellation (PIC) with maximum ratio combining (MRC) technology is proposed to use for receiver to combat the intersymbol interference (ISI) problem over multipath fading channel. With the aid of MRC scheme, the proposed partial PIC technique can effectively perform the interference cancellation and acquire the benefit of time diversity gain. Finally, the proposed system can be extended to use for multiple antenna systems to provide excellent performance. Simulation results reveal that the proposed low complexity partial PIC-MRC SIMO system can provide robust performance and outperform the conventional PIC and the iterative frequency domain decision feedback equalizer (FD-DFE) systems over multipath fading channel environment.

1. Introduction

Over past decade, orthogonal frequency-division multiplexing (OFDM) system has become one of the most popular systems in wireless communication. This technique is seen today as a strong candidate for future generations of cellular mobile networks, but it involves the problem of high peak-to-average power ratio (PAPR), it will cause power amplifier working in the nonlinear area. Thus, it needs to back off output power which will reduce the efficiency of power amplifier. For single carrier block transmission (SCBT) system, it is the one of the popular themes in recent years [1–6]. It can provide low PAPR performance, so we try to study the interference cancellation technique to provide the excellent bit error rate (BER) performance and reduce the computation complexity at receiver.

References [2, 3] with the iterative frequency domain decision feedback equalizer (FD-DFE) are proposed for SCBT system. It is noted that the decision and iteration of the FD-DFE scheme are processed on frequency domain. And after more iteration, the performance of BER is improved obviously. Moreover, the BER performance of these systems is performed obviously only when the iterations number is enough high. However, large number of iterations will induce high complexity at the receiver. Parallel interference cancellation (PIC) scheme in [7–10] can overcome the intersymbol interference (ISI) problem effectively and improve the BER performance obviously. However, the BER performance is worse than FD-DFE in [3] even use more iteration loops.

Therefore, in order to alleviate the above problem, the partial PIC with maximum ratio combing (MRC) technique is proposed in this paper. That is, with the aid of MRC scheme [11], the proposed partial PIC technique can effectively perform the interference cancellation and acquire the benefit of time diversity gain. In fact, with more taps for weighting combination, it will lead to higher time diversity gain. Furthermore, it indicates that the proposed technique can achieve better BER due to the diversity gain. This can mainly be attributed to the ability of this scheme to effectively deal with interference effects and achieve inherent time diversity with MRC. And it also can extend to multiple

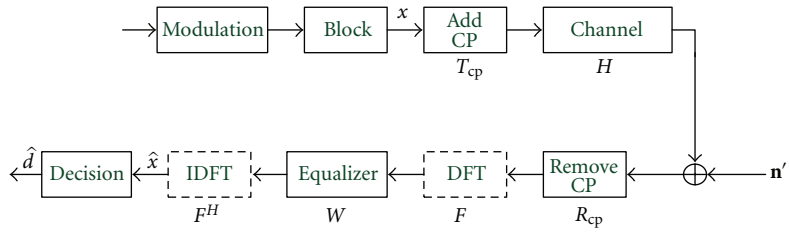

Figure 1: Block diagram of SCBT system.

antenna system and obtain further performance. Moreover, the antenna selection technique (AST) [12–15] is used to reduce the cost and power associated with the single input multiple output (SIMO) system. Simulation results reveal that the proposed low complexity partial PIC-MRC system can provide lower receiver complexity and robust performance than the conventional PIC and the iterative FD-DFE systems over multipath fading channel environment.

The remainder of this paper is organized as follows: Section 2 introduces the system model and the FD-DFE for the SCBT systems. In Section 3, PIC algorithm is used to cancel the block interference, and iterative partial PIC-MRC scheme is proposed to enhance BER performance further. In Section 4, the proposed system is extended to the multiple antenna system. Results of performance tests of the proposed system are then given in Section 5, and Section 6 concludes the study.

2. System Model

2.1. Frequency Domain Equalization System. Figure 1 shows a basic configuration of the SCBT system. First the nth information signal block of size $N \times 1$ can be defined as $\mathbf{x}(n) = [x_0(n), \ldots, x_{N-1}(n)]^T$, where the superscript $(\cdot)^T$ stands for the transpose. The transmitted signal block of size $(N+K)\times 1$ is generated from $\mathbf{x}(n)$ by adding the cyclic prefix (CP) of K symbols length as the guard interval (GI). T_{cp} donates the CP insertion matrix of size $(N+K)\times N$ defined as

$$\mathbf{T}_{\text{cp}} = \begin{bmatrix} \mathbf{O}_{K\times(N-K)} & \mathbf{I}_K \\ & \mathbf{I}_N \end{bmatrix}_{(N+K)\times N}. \tag{1}$$

$\mathbf{O}_{K\times(N-K)}$ is a zero matrix of size $K \times (N-K)$, and $\mathbf{I}_N$ is an identity matrix of size $N \times N$. The received signal block $\hat{\mathbf{y}}(n)$ is written as

$$\hat{\mathbf{y}}(n) = \mathbf{H}\mathbf{T}_{\text{cp}}\mathbf{x}(n) + \mathbf{n}'(n) = \mathbf{h}\otimes_c \hat{\mathbf{x}}(n) + \mathbf{n}'(n), \tag{2}$$

where $\mathbf{n}'(n)$ is a channel noise vector of size $(N+K)\times 1$. $\otimes_c$ represents as circular convolution and $\mathbf{h} = \{h_0, \ldots, h_{G-1}\}$ denotes the channel impulse response which can arrange the Toeplitz channel matrices $\mathbf{H}$ of size $(N+K)\times(N+K)$, and G is the length of multipath. After discarding the CP portion of the received signal block, the received signal block $\mathbf{y}(n)$ of size $N \times 1$ can be written as

$$\mathbf{y}(n) = \mathbf{R}_{\text{cp}}\mathbf{H}\mathbf{T}_{\text{cp}}\mathbf{x}(n) + \mathbf{n}(n), \tag{3}$$

where $\mathbf{R}_{\text{cp}}$ denotes the CP discarding matrix of size $N \times (N+K)$ defined as

$$\mathbf{R}_{\text{cp}} = \begin{bmatrix} \mathbf{O}_{N\times K} & \mathbf{I}_N \end{bmatrix}_{N\times(N+K)} \tag{4}$$

and $\mathbf{n}(n) = \mathbf{R}_{\text{cp}}\mathbf{n}'(n)$. Next, after CP insertion and discarding CP portion, the channel matrix $\mathbf{H}$ will be changed into a circulant matrix $\mathbf{H}_c$ of size $N \times N$, which can be written as

$$\mathbf{H}_c = \mathbf{R}_{\text{cp}}\mathbf{H}\mathbf{T}_{\text{cp}} = \mathbf{F}^H\mathbf{\Lambda}\mathbf{F}, \tag{5}$$

where $\mathbf{\Lambda}$ is the frequency-domain channel response, and $\mathbf{F}$ is defined as a discrete Fourier transform (DFT) matrix. After DFT, frequency domain equalizer $\mathbf{W}$ and IDFT are processing, the equalized signal can be written as

$$\hat{\mathbf{x}}(n) = \mathbf{F}^H\mathbf{W}\mathbf{\Lambda}\mathbf{F}\mathbf{x}(n) + \mathbf{F}^H\mathbf{W}\mathbf{F}\mathbf{n}(n), \tag{6}$$

where $(\cdot)^H$ stands for the conjugate transpose. The equalizer consists of zero-forcing (ZF) and minimum mean square error (MMSE) equalizers, where ZF is defined as $\mathbf{W}_{\text{ZF}} = \mathbf{\Lambda}^{-1}$ and MMSE is defined as $\mathbf{W}_{\text{MMSE}} = \left(\mathbf{\Lambda}^H\mathbf{\Lambda} + \sigma_n^2/\sigma_x^2\mathbf{I}_N\right)^{-1}\mathbf{\Lambda}^H$, and σ_n^2 and σ_x^2 are the variance of noise and signal. The equalized signal can be rewritten as

$$\begin{aligned}\hat{\mathbf{x}}(n) &= \mathbf{F}^H\mathbf{W}_{\text{MMSE}}\mathbf{F}\mathbf{H}_c\mathbf{x}(n) + \mathbf{F}^H\mathbf{W}_{\text{MMSE}}\mathbf{F}\mathbf{n}(n) \\ &= \overline{\mathbf{H}}\mathbf{x}(n) + \mathbf{F}^H\mathbf{W}_{\text{MMSE}}\mathbf{F}\mathbf{n}(n),\end{aligned} \tag{7}$$

where $\overline{\mathbf{H}} = \mathbf{F}^H\mathbf{W}_{\text{MMSE}}\mathbf{F}\mathbf{H}_c$, and $\overline{\mathbf{H}}$ is a new channel matrix of size $N \times N$. In Figure 3, the energy of $\overline{\mathbf{H}}$ is concentrated on the diagonal, but there still have residue ISI, which will degrade the system performance. So interference cancellation systems are proposed to cancel the ISI and achieve better performance.

2.2. Frequency-Domain Decision Feedback Equalizer

2.2.1. Iterative MMSE Decision Feedback Equalizer. Figure 2 shows a bock diagram of FD-DFE system, suppose that the received block is fed to the DFT operator, whose output block is denoted as $(Y_0, Y_1, \ldots, Y_{N-1})$. The equalizer multiplies this signal block with its feedforward coefficients $(F_0, F_1, \ldots, F_{N-1})$, and the resulting signal block enters an inverse DFT, which yields the output block $(\hat{x}_0, \hat{x}_1, \ldots, \hat{x}_{N-1})$ on which the threshold detector bases its first decisions for the transmitted signal block.

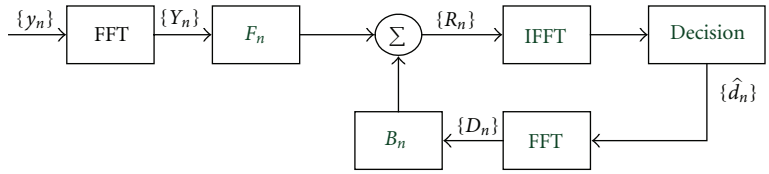

Figure 2: Block diagram of iterative FD-DFE.

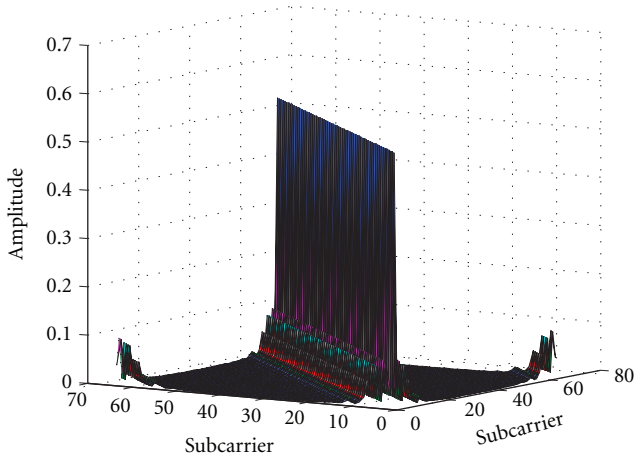

Figure 3: The characteristics of time domain channel matrix $\overline{\mathbf{H}}$.

Once the receiver makes a first set of decisions, the decision block is fed to a feedback filter with coefficients $(B_0, B_1, \ldots, B_{N-1})$, and an iterative DFE is implemented. At the lth iteration, the feedforward and feedback filter block supplies

$$R_n(l) = F_n(l)Y_n + B_n(l)D_n(l-1), \quad n = 0, 1, \ldots, N-1, \tag{8}$$

where the $F_n(l)$ and $B_n(l)$ coefficient sets are, respectively, the feedforward and feedback filter coefficients at the lth iteration, and the $D_n(l-1)$ is the frequency-domain decisions at the previous iteration. The initial MMSE equalizer is given as

$$F_n(0) = \frac{\Lambda_n^*}{\sigma_n^2/\sigma_x^2 + (|\Lambda_n|)^2}, \quad n = 0, 1, \ldots, N-1, \tag{9}$$

where Λ_n is frequency-domain channel response, and initial feedback filter coefficient is given as

$$B_n(0) = 0. \tag{10}$$

The first equalizer decisions are obtained using $\alpha_0 = 1$, and the definition of α_k is given in [4]

$$\alpha_l = 1 - \frac{\sqrt{l}}{\sqrt[10]{L}}, \tag{11}$$

where L is the number of iterations. At the lth iteration, the feedforward and the feedback filter coefficients are, respectively, given by

$$F_n(l) = \frac{\Lambda_n^*}{\sigma_n^2/\sigma_x^2 + \left(1 - \alpha_{l-1}^2\right)|\Lambda_n|^2},$$
$$B_n(l) = \alpha_{l-1}\left[\Lambda_n F_n(l) - \frac{1}{N}\sum_{n=1}^{N}\Lambda_n F_n(l)\right]. \tag{12}$$

2.2.2. Iterative MF-Based Decision Feedback Equalizer. In the iterative DFE proposed in [5], the feedforward filter in that DFE shifts linearly from a linear MMSE filter at the first $(L-1)$ iterations to the matched filter (MF) at the last iteration. At the lth iteration, the feedforward and the feedback filter coefficients are, respectively, given by

$$F_n(l) = \alpha_l \frac{\Lambda_n^*}{\sigma_n^2/\sigma_x^2 + |\Lambda_n|^2} + (1-\alpha_l)\Lambda_n^*,$$
$$B_n(l) = 1 - F_n(l)\Lambda_n. \tag{13}$$

The first equalizer decisions are obtained using $\alpha_0 = 1$ that is, the equalizer is clearly a linear MMSE equalizer. Then, the α_l parameter decreases linearly as

$$\alpha_l = 1 - \frac{l}{L}. \tag{14}$$

At the last iteration, $\alpha_l = 0$, and the feedforward filter becomes an MF.

3. Parallel Interference Cancellation

The residue ISI will degrade the system performance. Thus, in this section, the PIC is used to cancel the ICI problems in SCBT system.

3.1. Conventional Parallel Interference Cancellation. Figure 4 is the schematic diagram of interference, the colored boxes are interference in the received symbols. $\overline{H}_{i,d}$ is expressed as the dth symbol data to the ith interference symbol. When i is different from d, that is, $i \neq d, \overline{H}_{i,d}x(n)$ is the ISI which will degrade the system performance. Figure 5 is the block diagram of PIC in SCBT system. $\widetilde{x}_n$ is the equalized signal $\hat{x}_n$ in (7) after canceling the ISI, which can be given as

$$\widetilde{x}_n = \left(\hat{x}_n - \left(\overline{\mathbf{h}}_n - \mathbf{h}_n\right)\left(\widetilde{\mathbf{d}} - \widetilde{\mathbf{d}}_n\right)\right)\overline{H}_{n,n}^{-1}, \tag{15}$$

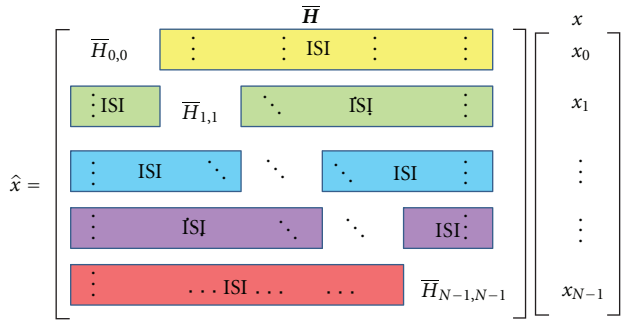

Figure 4: Schematic diagram of intersymbol interference.

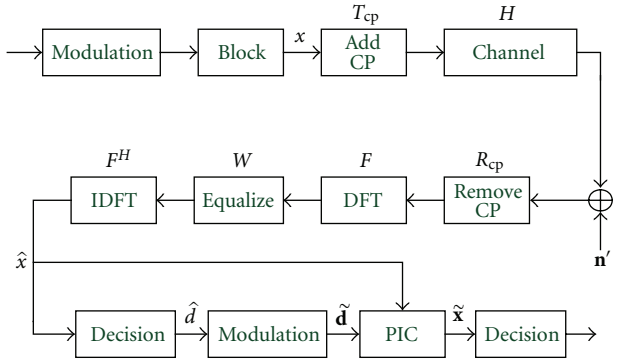

Figure 5: Block diagram of PIC in SCBT system.

where $\overline{\mathbf{h}}_n$ is the $(n+1)$th row vector of $\overline{\mathbf{H}}$, and $\mathbf{h}_n$ is defined as $\mathbf{h}_n = [\,\mathbf{0}_{1\times n}\ \overline{H}_{n,n}\ \mathbf{0}_{1\times(N-n-1)}\,]$, $\tilde{\mathbf{d}}$ is the modulated signal of QPSK after the decision

$$\tilde{\mathbf{d}} = \left[\tilde{d}_0\ \ \tilde{d}_1\ \ \cdots\ \ \tilde{d}_{N-1}\right]^T \tag{16}$$

and $\tilde{\mathbf{d}}_n$ is defined as

$$\tilde{\mathbf{d}}_n = \left[\mathbf{0}_{1\times n}\ \ \tilde{d}_n\ \ \mathbf{0}_{1\times(N-n-1)}\right]^T. \tag{17}$$

After canceling the ISI terms, the interference cancelled signal $\tilde{\mathbf{x}}$ can be detected by the decision operation.

3.2. Partial PIC with Maximum Ratio Combining. PIC algorithm can overcome the ISI problem effectively and improve the BER performance obviously. However, as shown in (15) for only one-tap equalizer, it will result in the loss of energy for the symbol detection. Besides, in order to enhance the receiver performance in Section 3.1, the number of iterations needs to be increased. It will induce more computation complexity. Therefore, in order to alleviate the above problem, the partial PIC with maximum ratio combing technique is proposed in this paper. That is, with the aid of MRC scheme, the proposed partial PIC technique can effectively perform the interference cancellation and acquire the benefit of time diversity gain. In fact, with more taps for weighting combination, it will lead to higher time diversity gain. Furthermore, it indicates that the proposed technique can achieve better BER due to the diversity gain.

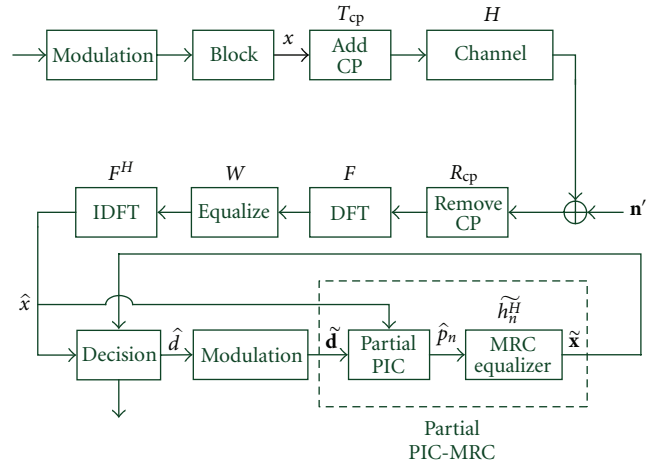

Figure 6: Block diagram of iterative partial PIC-MRC in SCBT system.

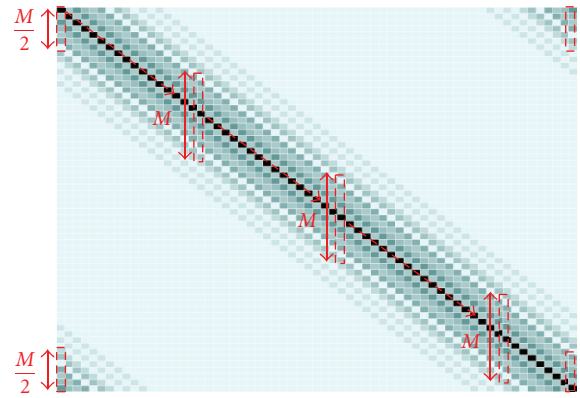

Figure 7: The illustration of partial selection matrix for partial PIC-MRC.

This can mainly be attributed to the ability of this scheme to effectively deal with interference effects and achieve inherent time diversity with MRC.

The block diagram is shown in Figure 6 and the illustration of partial PIC is shown in Figure 7. Its structure is similar to PIC. The main difference is that PIC-MRC doing partial PIC first and then combines the partial energy from other received symbols by MRC algorithm. Finally, using the MRC equalizer can obtain the detected signal. To simplify the exposition, we consider a simple case. First, from (7) and (15), the partial parallel interference is reconstructed by $\mathbf{G}_0(\overline{\mathbf{H}} - \overline{\mathbf{H}}_0)(\tilde{\mathbf{d}} - \tilde{\mathbf{d}}_0)$, where $\mathbf{G}_0$ is the partial selection matrix of parallel interference with window size M selection, that is, $\mathbf{G}_0 = [\,[\mathbf{I}_{M/2\times M/2}\mathbf{0}_{M/2\times M/2}]^T\ \mathbf{0}_{M\times(N-M)}\ [\mathbf{0}_{M/2\times M/2}\mathbf{I}_{M/2\times M/2}]^T\,]$ with the identity matrix $\mathbf{I}_{M/2\times M/2}$, the zero matrices $\mathbf{0}_{M\times(N-M)}$ and $\mathbf{0}_{M/2\times M/2}$. Next, the received partial signal $\mathbf{G}_0\hat{\mathbf{x}}$ can be

subtracted by the partial parallel interference. The residual signal can be expressed by

$$\hat{\mathbf{p}}_0 = \mathbf{G}_0\hat{\mathbf{x}} - \mathbf{G}_0\left(\overline{\mathbf{H}} - \overline{\mathbf{H}}_0\right)\left(\tilde{\mathbf{d}} - \tilde{\mathbf{d}}_0\right), \tag{18}$$

where $\overline{\mathbf{H}}_0 = \left[\tilde{\mathbf{h}}_0\ \mathbf{0}_{N\times(N-1)}\right]$, $\tilde{\mathbf{d}}$ and $\tilde{\mathbf{d}}_0$ are the modulated signal after decision in (16)-(17), and $\tilde{\mathbf{h}}_0$ is the first column vector of $\overline{\mathbf{H}}$. After MRC operation, the detected signal can be obtained by the MRC equalization

$$\tilde{x}_0 = \frac{\tilde{\mathbf{h}}_0^H\mathbf{G}_0\left(\hat{\mathbf{x}} - \left(\overline{\mathbf{H}} - \overline{\mathbf{H}}_0\right)\left(\tilde{\mathbf{d}} - \tilde{\mathbf{d}}_0\right)\right)}{\left\|\mathbf{G}_0\tilde{\mathbf{h}}_0\right\|^2}. \tag{19}$$

Similarly to the procedures of (18) and (19), the nth partial PIC-MRC signal can be obtained by

$$\tilde{x}_n = \frac{\tilde{\mathbf{h}}_n^H\mathbf{G}_n\left(\hat{\mathbf{x}} - \left(\overline{\mathbf{H}} - \overline{\mathbf{H}}_n\right)\left(\tilde{\mathbf{d}} - \tilde{\mathbf{d}}_n\right)\right)}{\left\|\mathbf{G}_n\tilde{\mathbf{h}}_n\right\|^2}, \tag{20}$$

where $\overline{\mathbf{H}}_n = \left[\mathbf{0}_{N\times n}\ \tilde{\mathbf{h}}_n\ \mathbf{0}_{N\times(N-n-1)}\right]$, $\tilde{\mathbf{h}}_n$ is the $(n+1)$th column vector of $\overline{\mathbf{H}}$, and the partial selection matrix $\mathbf{G}_n$ is

$$\mathbf{G}_n = \begin{cases} \left[\left[\mathbf{I}_{(M/2+n)\times(M/2+n)}\ \ \mathbf{0}_{(M/2-n)\times(M/2+n)}\right]^T\ \ \mathbf{0}_{M\times(N-M)}\ \ \left[\mathbf{0}_{(M/2+n)\times(M/2-n)}\ \ \mathbf{I}_{(M/2-n)\times(M/2-n)}\right]^T\right], & \text{if } n < \dfrac{M}{2} \\ \left[\mathbf{0}_{M\times(n-M/2)}\ \ \mathbf{I}_{M\times M}\ \ \mathbf{0}_{M\times(N-M/2-n)}\right], & \text{if } n \geq \dfrac{M}{2},\ n \leq N - \dfrac{M}{2} \\ \left[\left[\mathbf{I}_{(M/2+n-N)\times(M/2+n-N)}\ \ \mathbf{0}_{(M/2-n+N)\times(M/2+n-N)}\right]^T\ \ \mathbf{0}_{M\times(N-M)}\ \ \left[\mathbf{0}_{(M/2+n-N)\times(M/2-n+N)}\ \ \mathbf{I}_{(M/2-n-N)\times(M/2-n+N)}\right]^T\right] & \text{if } n > N - \dfrac{M}{2}. \end{cases} \tag{21}$$

It is noteworthy that the equalizers in (19) and (20) are still one-tap equalizer with low complexity, which do not induce noise enhancement problem due to $\|\mathbf{G}_n\tilde{\mathbf{h}}_n\|^2$ with the robust summarized channel responses. The partial PIC-MRC algorithm not only can acquire time diversity gain, but also reduce the computation complexity than the conventional PIC scheme in Section 3.1 because it needs more iteration loops to enhance performance at receiver side.

4. Partial PIC-MRC SIMO System

In this section, the proposed partial PIC-MRC system is extended into multiple antenna systems.

4.1. Partial PIC-MRC SIMO System. The advantage of SIMO systems is that better BER performance can be achieved without using any additional transmit power and bandwidth. The SIMO system with one transmit and N_R receive antennas is shown in Figure 8. At each receive antenna, the same procedures of equalizer are processed, for example, frequency domain equalization and partial PIC-MRC operation with iteration number L. Finally, the decision scheme is used to detect the combination signal from the N_R equalizers.

4.2. Antenna Selection Technique. Although the SIMO system in Section 4.1 can provide better BER performance than the conventional single input single output (SISO) antenna system, the main drawback of the SIMO system is the requirement of the additional high-cost radio frequency (RF) modules. RF module includes low noise amplifier, mixer, band pass filter, low pass filter, and analog-to-digital converter. For multiple RF modules in SIMO system, the higher cost and power consumption are needed. In order to reduce the cost and power associated with the SIMO system, the antenna selection technique is used in the proposed SIMO system, that is, the number of the receive antenna being larger than the RF modules. Figure 9 is the block diagram of antenna selection technique (AST) in which only Q RF modules are used to support N_R receive antennas.

To do the AST algorithm, we first use the channel capacity algorithm, that is,

$$C^i = \log_2\det\left(\mathbf{I}_N + \frac{\sigma_x^2}{\sigma_n^2}\mathbf{H}_c^i\mathbf{H}_c^{iH}\right), \quad i = 1,\ldots,N_R, \tag{22}$$

where $\mathbf{H}_c^i$ is the channel matrix of the selected ith receive antenna. Next, based on the different combination of channel matrix, the AST algorithm finally chooses the Q receive antennas, which can provide the maximum channel capacity C^i to use for the proposed SIMO system.

5. Simulation Results

In this section, simulation results are conducted to demonstrate the performance of the proposed partial PIC-MRC system, and Table 1 is the system parameter settings. Perfect channel state information is assumed for simulation.

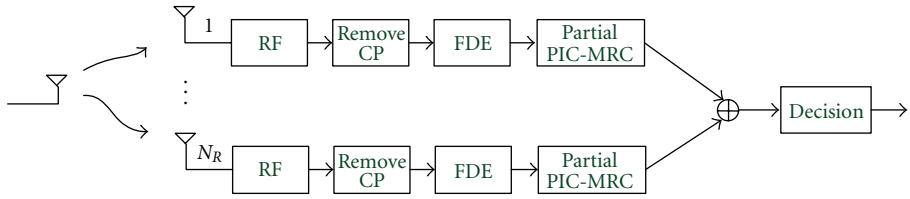

Figure 8: Block diagram of the partial PIC-MRC SIMO SCBT system.

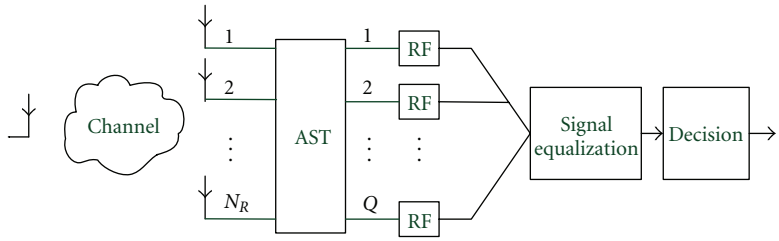

Figure 9: The structure of antenna selection with Q RF modules and N_R receive antennas.

Table 1: System simulated parameters.

Parameter	Specification
Modulation type	QPSK
FFT length (N)	64
Multipath number	6
Channel model	Equal gain rayleigh fading channel
CP length	16

Figure 10 shows the BER performance of iterative MMSE decision feedback equalizer and iterative MF-based decision feedback equalizer. The number of iteration is 2, 4, and 6 times. As shown in Figure 10, the system performance is better as the number of iteration increases. Besides, for the iteration number being 2, the performance of the iterative MMSE FDE can approach to the MMSE equalizer. At the iteration number being 4 and 6, the performance of the iterative MMSE FDE increases about 1 dB and 1.5 dB than MMSE equalizer at BER $= 4 \times 10^{-5}$, respectively. When the number of iteration is 6, the performance of iterative MMSE DFE is better than the iterative MF-based DFE receiver about 1.4 dB at BER $= 2 \times 10^{-5}$.

For partial PIC-MRC in SCBT system, the window size M in (18)–(20) can be selected by the simulation result which is shown in Figure 11. It is obviously that when M is larger than 16 under different E_b/N_0, the performance will achieve to the bound of full PIC-MRC system. Therefore, on the basis of the result, the size of the window $M = 16$ will be utilized for the following simulations.

Figure 12 shows the BER performance of PIC and partial PIC-MRC in SCBT system. The dotted lines are the best performance bound of PIC and partial PIC-MRC, respectively. Note that the bound performance is evaluated for the assumption of the perfect signal detection used for PIC cancellation. Next, we can see that the performance of the proposed partial PIC-MRC scheme is better than the

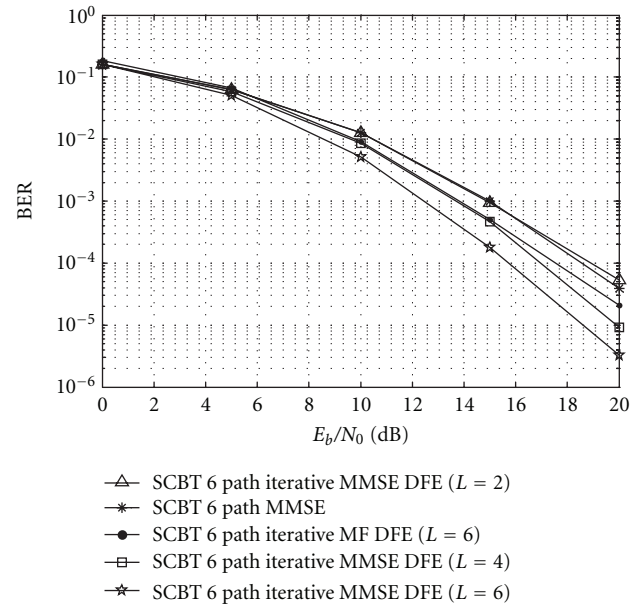

Figure 10: BER performance of iterative MMSE/MF-based DFE.

conventional PIC scheme about 1 dB at BER $= 10^{-5}$, but the performance is lower than iterative MMSE DFE ($L = 6$) about 0.6 dB.

Next, the BER performance is evaluated for the iterative partial PIC-MRC and MMSE DFE systems. As shown in Figure 13, after more iteration, the performance of the proposed partial PIC-MRC system has increased obviously. After 2 iterations, the performance has been better than the iterative MMSE DFE system 0.6 dB at BER $= 4 \times 10^{-6}$, and then the performance increases again about 0.2 dB after 3 iterations. From above simulation results, the proposed iterative partial PIC-MRC scheme in SCBT system can actually acquire better BER performance and provide low complexity

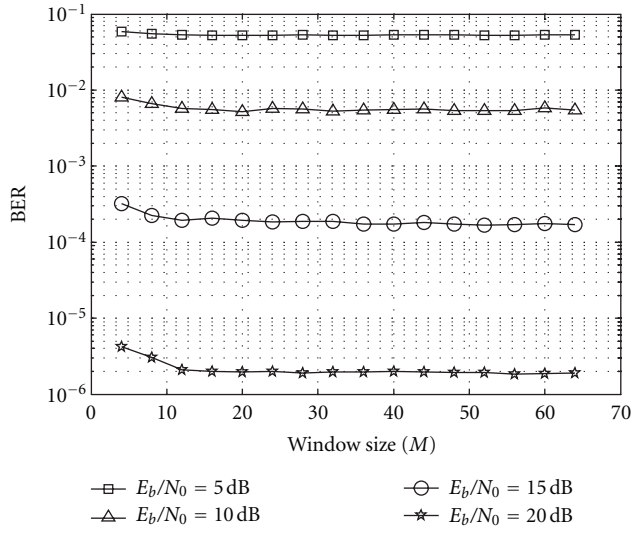

Figure 11: BER performance partial PIC-MRC under different window size M in SCBT system.

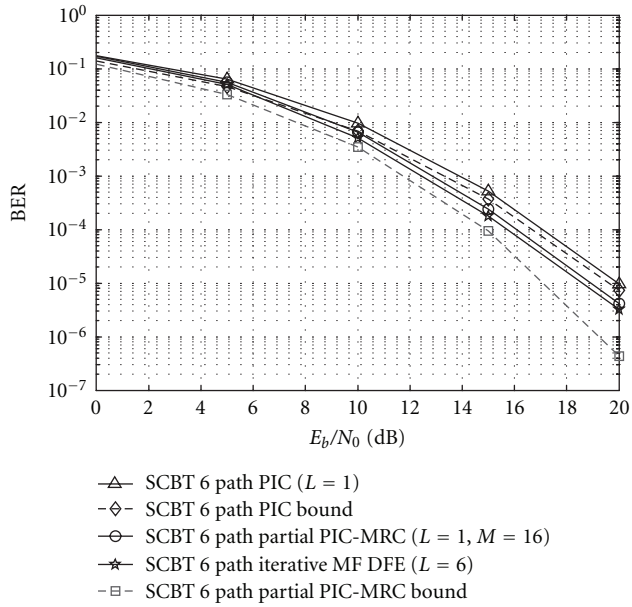

Figure 12: BER performance of PIC, partial PIC-MRC, and MMSE-DFE in SCBT system.

computation. For the computation complexity in Figure 13, the number of complex multiplication of the iterative MMSE DFE ($L = 6$) is computed about $O(3LN \log_2 N + 7NL)$ due to the iterative DFE-MMSE weight operation. Next, for the proposed partial PIC-MRC scheme in (19)-(20), it involves the advantage of $\tilde{\mathbf{d}}$ with the fixed values (i.e., QPSK symbol: $\pm 1 \pm j$). Therefore, it does not need complex multiplication for the parallel interference reconstruction. Furthermore, the number of complex multiplication of the proposed partial PIC-MRC ($L = 3$) can be computed about $O(2N \log_2 N + 2N + 2ML)$. For example, considering the iterative MMSE DFE system in Figure 13 with $L = 6$ and $N = 64$, the number

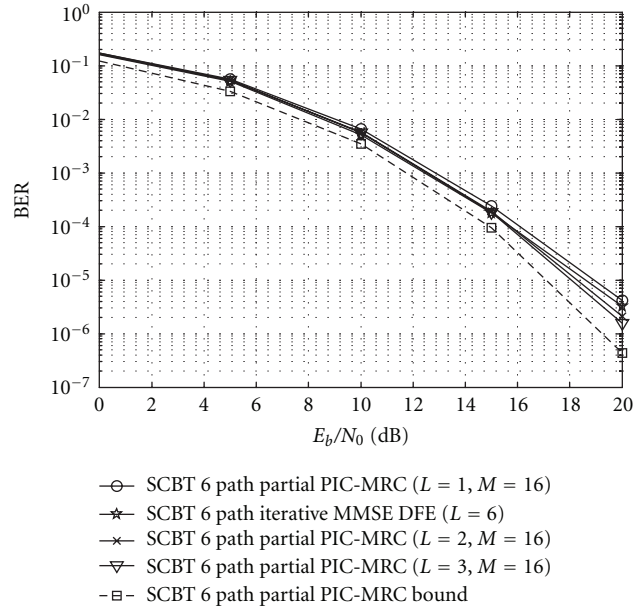

Figure 13: BER performance of iterative partial PIC-MRC and MMSE-DFE in SCBT system.

of complex multiplication is about 9600. And considering the proposed partial PIC-MRC system in Figure 13 with $L = 3$, $M = 16$, and $N = 64$, the number of complex multiplication is about 992. It is obvious that the proposed scheme with the lower window size M and iteration size L can provide the advantage of the lower computation complexity.

Finally, the proposed system is extended to multiple antenna system. Figure 14 shows the BER performance of the proposed partial PIC-MRC SIMO systems with the receive antenna number from 2 to 4. With more receive antennas, the BER performance is shown better obviously. And Figure 15 is the BER performance of the proposed AST technique in the partial PIC-MRC SIMO system. Assume the RF modules Q is one and total receive antenna number is from 2 to 4. If antenna number equals to 2, the performance increases about 3 dB at BER $= 10^{-5}$ than SISO system. When the receive antenna number equals to 4, the performance almost achieves the SIMO system with one tranmit antenna and two receive antennas at $E_b/N_0 = 14$ dB. Note that the proposed AST system with low cost and power benefit is due to the RF module $Q = 1$ and the receive antenna number $N_R = 4$, where RF module of the proposed scheme is smaller than the RF modules $Q = 2$ of the SIMO system. It is noteworthy that the proposed SIMO PIC-MRC system with AST algorithm under $Q = 1$ and $N_R = 4$ scenario is the SISO system with single RF and multiple antennas for selection. Therefore, in this scenario, the proposed AST SIMO system is still a SISO system with multiple antenna extension. Next, as shown in Figure 15, the proposed AST SIMO system can approach to the BER performance of the SIMO system with $Q = 2$ (two RFs). Therefore, the proposed AST SIMO system involves the advantage of the flexible structure of multiple antennas and RFs selection.

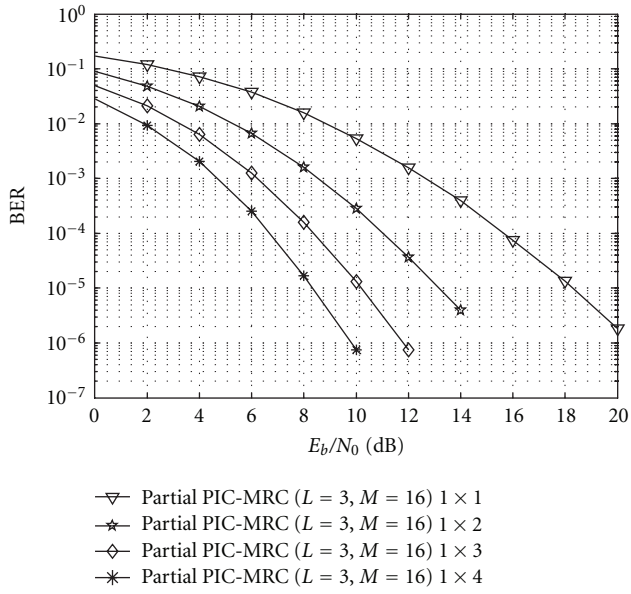

Figure 14: BER performance of partial PIC-MRC SIMO systems.

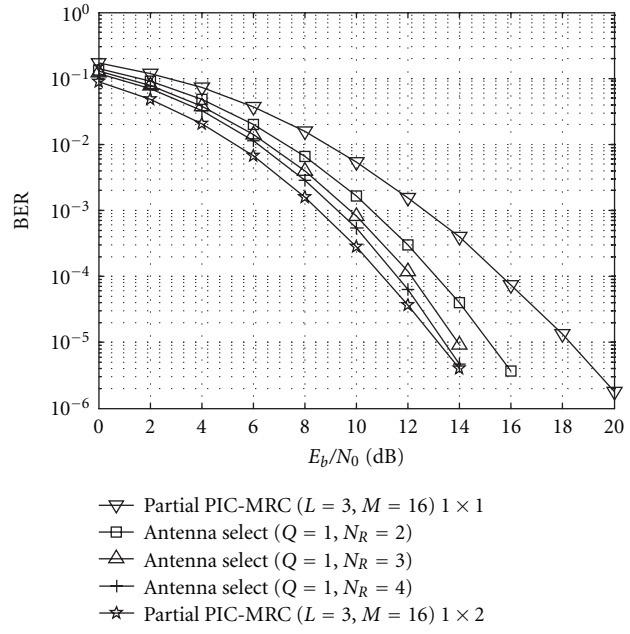

Figure 15: BER performance of partial PIC-MRC with antenna selection technique.

6. Conclusions

The partial PIC-MRC system is proposed for SCBT system, which is in order to achieve better BER performance and low complexity at the receiver side. With the aid of MRC scheme, the proposed partial PIC technique can effectively perform the interference cancellation and acquire the benefit of time diversity gain, which can achieve better BER performance. And it also can extend to multiple antenna structure with better BER performance. AST will introduce the select diversity and reduce the cost and power consumption of the SIMO system. Simulation results confirm that the proposed partial PIC-MRC SIMO system with the AST scheme can provide robust performance over multipath fading channel environment.

Acknowledgments

The authors would like to thank the National Science Council of the Republic of China, Taiwan, for financially supporting this research under Contract no. NSC 100-2220-E-155-006 and NSC 101-2220-E-155-006. The authors also thank the editor and anonymous reviewers for their helpful comments and suggestions in improving the quality of this paper.

References

[1] Z. Wang, X. Ma, and G. B. Giannakis, "OFDM or single-carrier block transmissions?" *IEEE Transactions on Communications*, vol. 52, no. 3, pp. 380–394, 2004.

[2] F. Sainte-Agathe and H. Sari, "Single-Carrier transmission with frequency-domain decision-feedback equalization," in *Proceedings of the 13th European Signal Processing Conference (EUSIPCO '05)*, Antalya, Turkey, September 2005.

[3] N. Benvenuto and S. Tomasin, "Block iterative DFE for single carrier modulation," *Electronics Letters*, vol. 38, no. 19, pp. 1144–1145, 2002.

[4] N. Benvenuto and S. Tomasin, "On the comparison between OFDM and single carrier modulation with a DFE using a frequency-domain feedforward filter," *IEEE Transactions on Communications*, vol. 50, no. 6, pp. 947–955, 2002.

[5] D. Falconer, S. L. Ariyavisitakul, A. Benyamin-Seeyar, and B. Eidson, "Frequency domain equalization for single-carrier broadband wireless systems," *IEEE Communications Magazine*, vol. 40, no. 4, pp. 58–66, 2002.

[6] Z. Wang and G. B. Giannakis, "Wireless multicarrier communications: where Fourier meets Shannon," *IEEE Signal Processing Magazine*, vol. 17, no. 3, pp. 29–48, 2000.

[7] T. K. Moon and W. C. Stirling, *Mathematical Methods and Algorithm for Signal Processing*, Prentice-Hall, Englewood Cliffs, NJ, USA, 2000.

[8] S. Tomasin, A. Gorokhov, H. Yang, and J. P. Linnartz, "Iterative interference cancellation and channel estimation for mobile OFDM," *IEEE Transactions on Wireless Communications*, vol. 4, no. 1, pp. 238–245, 2005.

[9] F. Siddiqui, F. Danilo-Lemoine, and D. Falconer, "PIC assisted IBDFE based iterative spatial channel estimation with intra and inter-cell interference in SC-FDE system," in *2007 IEEE 66th Vehicular Technology Conference, VTC 2007-Fall*, pp. 501–505, usa, October 2007.

[10] F. Siddiqui, F. Danilo-Lemoine, and D. Falconer, "Iterative interference cancellation and channel estimation for mobile SC-FDE systems," *IEEE Communications Letters*, vol. 12, no. 10, pp. 746–748, 2008.

[11] T. Kumagai, M. Mizoguchi, T. Onizawa, H. Takanashi, and M. Morikura, "Maximal ratio combining frequency diversity ARQ scheme for OFDM signals," in *Proceedings of the 9th IEEE International Symposium on Personal, Indoor and Mobile Radio Communications (PIMRC '98)*, pp. 528–532, September 1998.

[12] E. Telatar, "Capacity of multi-antenna Gaussian channels," *European Transactions on Telecommunications*, vol. 10, no. 6, pp. 585–595, 1999.

[13] A. Gorokhov, "Antenna selection algorithms for MEA transmission systems," in *2002 IEEE International Conference on Acoustic, Speech, and Signal Processing*, pp. III/2857–III/2860, usa, May 2002.

[14] A. Gorokhov, D. A. Gore, and A. J. Paulraj, "Receive antenna selection for MIMO spatial multiplexing: theory and algorithms," *IEEE Transactions on Signal Processing*, vol. 51, no. 11, pp. 2796–2807, 2003.

[15] A. F. Molisch and M. Z. Win, "Mimo systems with antenna selection," *IEEE Microwave Magazine*, vol. 5, no. 1, pp. 46–56, 2004.